

## Double-balanced bridge circuit – simulation studies

**Abstract.** The article presents simulation studies of the double-balancing bridge circuit intended for measurements of the dielectric loss factor ( $\tan \delta$ ). A characteristic feature of the bridge is the need to perform two balancing steps and balancing the voltage modules of selected circuit's voltages. The advantage of the bridge is a very simple design and no problem with convergence. Double balance bridge system – simulation tests.

**Streszczenie.** W artykule zaprezentowano badania symulacyjne układu mostka z podwójnym równoważeniem przeznaczonego do pomiarów współczynnika strat dielektrycznych. Charakterystyczną cechą mostka jest konieczność wykonania dwóch kroków równoważenia oraz równoważenie modułów napięć wyróżnionych układu. Zaletą układu jest bardzo prosta konstrukcja i brak problemu ze zbieżnością. Układ mostkowy z podwójnym równoważeniem – badania symulacyjne. (Układ mostkowy z podwójnym równoważeniem – badania symulacyjne)

**Keywords:** impedance components measuring, loss factor measuring, AC bridges, bridge convergence

**Słowa kluczowe:** pomiar składowych impedancji, pomiar współczynnika strat dielektrycznych, mostki AC, zbieżność mostków

### Introduction

Measuring circuits designed to measure impedance components are used to determine electrical parameters of binaries, such as resistance, capacitance, or inductance. They are also used to measure coefficients that are the relation of impedance components, e.g. goodness of coils or the dielectric loss coefficient of loss capacitors. Such measurements provide information, for example, on the quality of insulation materials.

The choice of a measuring circuit to measure impedance components is determined primarily by the measuring range, accuracy, frequency, and effective value of the measuring voltage, the possibility of testing non-linear elements, and also the ease of automation of the circuit. Unfortunately, it is not possible to indicate universal measuring circuits whose metrological properties allow them to be used to study any object. That is why new measurement circuits are designed and researched, often returning to forgotten ideas. Such an example is the layout shown in Fig. 1, presented more than half a century [1]. It is a circuit with a bridge structure designed to measure the dielectric loss coefficient. The technology of that time significantly hindered the construction of such a circuit, primarily due to the properties of voltmeters built at that time.

### Principle of operation and balancing process

Fig. 1 shows the structure of the system and the characteristic points of the bridge. The object under test is a lossy capacitor modeled as a series RC connection. Two balancing steps are required in the measurement process. In both steps, the state to which the bridge is reduced is the state of equality of the modules of the corresponding voltages. This means that it is easy to detect highlighted states, for example, by measuring the effective value. Reducing to the highlighted states requires the use of two adjustable elements,  $R_p$  and  $R_{CC'}$ . Only one adjustable element is used in each measuring step; The setting of the first setting element obtained in the first step remains constant in the second step. The advantage of the presented system is a very simple design and constant maximum convergence. The system allows only the mutual relationship between the components to be measured.

In the layout from Fig. 1, typical bridge points ABCD and additionally points E and CC' are distinguished. The bridge in question is an unbalanced bridge because, from the point of view of the diagonal CD, it cannot be brought to a state of equilibrium. The system can be classified as quasi-balanced

systems with modular quasi-balancing.

A preliminary study of the properties of the system is presented in the paper [2]. The equation to determine the measured  $\tan \delta$  in the work [1] was derived on the basis of the analysis of the phase plot. Further measurement steps will be presented.

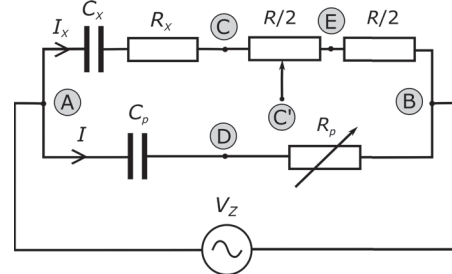


Fig. 1. Bridge system designed to measure dielectric loss coefficient

Fig. 2 shows the layout diagram in the first balancing step. The adjustable element here is the resistor  $R_p$ . When its settings, the  $V_{ED}$  voltage module is reduced to a value equal to the  $V_{EB}$  voltage modulus. The  $V_{EB}$  voltage in this step remains unchanged.

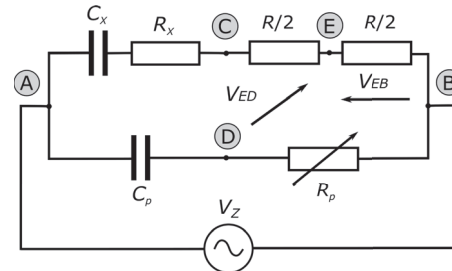


Fig. 2. Diagram of the system in the first balancing step

The  $V_{EB}$  voltage according to the above figure can be described as follows:

$$(1) \quad V_{EB} = \frac{V_Z}{Z_X + R} \cdot \frac{R}{2},$$

where

$$(2) \quad Z_X = R_X - j \frac{1}{\omega C_X}.$$

It can be seen that equation (1) is an example of a homograph function, known from the analysis of the balancing process of alternating current bridges [4]. The real parameter

of this function is the resistance  $R$ . The image of a function on the Gaussian plane is an arc passing through points A and B. The  $V_{EB}$  voltage has a fixed value because the supply voltage  $V_Z$ , resistance  $R$ , and impedance under test  $Z_X$  do not change during the measurement. A change in the  $R_p$  resistance does not affect the value of this voltage if the source of the supply voltage is a rigid source. The voltage modulus  $V_{EB}$  is equal to:

$$(3) \quad |V_{EB}| = \frac{|V_Z|}{2} \cdot \frac{R}{|Z_X + R|}.$$

The expression appearing in the denominator of equation (3) can be determined as

$$(4) \quad |Z_X + R| = \sqrt{(R_X + R)^2 + \left(\frac{1}{\omega C_X}\right)^2},$$

which allows to write the expression to the  $V_{EB}$  voltage module as follows:

$$(5) \quad |V_{EB}| = \frac{|V_Z|}{2} \cdot \frac{R}{\sqrt{(R_X + R)^2 + \left(\frac{1}{\omega C_X}\right)^2}}.$$

The  $V_{ED}$  voltage can be written as

$$(6) \quad V_{ED} = V_{EB} - V_{DB},$$

thus:

(7)

$$V_{ED} = \frac{V_Z}{Z_X + R} \cdot \frac{R}{2} - V_Z \cdot \frac{R_p}{Z_p} = \frac{V_Z}{2} \cdot \left[ \frac{R}{Z_X + R} - \frac{2R_p}{Z_p} \right],$$

where

$$(8) \quad Z_p = R_p - j \frac{1}{\omega C_p}.$$

The  $V_{ED}$  voltage module can be written as follows:

$$(9) \quad |V_{ED}| = \frac{|V_Z|}{2} \cdot \left| \frac{R}{Z_X + R} - \frac{2R_p}{Z_p} \right|.$$

Identifying the  $V_{ED}$  voltage module analytically is quite a problem. The calculation leads to the determination of the relationship shown below:

$$(10) \quad |V_{ED}| = \frac{|V_Z|}{2} \cdot \sqrt{\frac{R_p^2 \left[ (R + 2R_X)^2 + \left(\frac{4}{\omega C_X}\right)^2 \right] -}{R_p^2 \left[ (R_X + R)^2 + \left(\frac{1}{\omega C_X}\right)^2 \right] +} \dots} \\ \dots \frac{\dots R_p \left[ \frac{2R}{\omega^2 C_X C_p} \right] + \left(\frac{R}{\omega C_p}\right)^2}{\dots \left(\frac{1}{\omega C_p}\right)^2 \left[ (R_X + R)^2 + \left(\frac{1}{\omega C_X}\right)^2 \right]}$$

Equation (10) is complicated to analyze and makes it difficult to evaluate the properties of the system. In the first equilibrium state, the modules of the voltages  $V_{ED}$  and  $V_{EB}$  are equal to:

$$(11) \quad |V_{EB}| = |V_{ED}|.$$

Fig. 3 shows the layout diagram in the second balancing step. The adjustable element in this step is the resistor  $R_{CC'}$ . The

$R_p$  resistor setting remains unchanged, retaining the value of the first step. It can be seen that during the second measurement step, due to the constant resistance between points C and B of the bridge, the  $V_{CD}$  voltage remains constant.

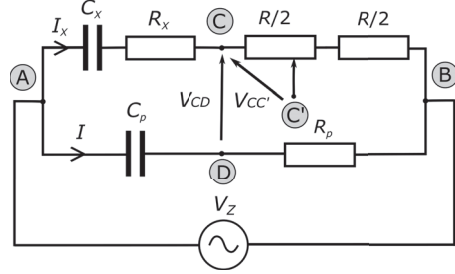


Fig. 3. Diagram of the circuit in the second balancing step

By changing the settings of the  $R_{CC'}$  resistor, the circuit is brought to a state in which the modules of the voltages  $V_{CC'}$  and  $V_{CD}$  are equal:

$$(12) \quad |V_{CD}| = |V_{CC'}|.$$

The voltage  $V_{CC'}$  is equal to:

$$(13) \quad V_{CC'} = I_X R_{CC'}, = \frac{V_Z}{Z_X + R} R_{CC'},$$

where current  $I_X$  is equal to

$$(14) \quad I_X = \frac{V_Z}{Z_X + R},$$

In turn, the  $V_{CD}$  voltage is described by the relationship

$$(15) \quad V_{CD} = V_{CB} - IR_p = \frac{V_Z}{Z_X + R} \cdot R - \frac{V_Z}{Z_p} R_p,$$

where current  $I$  is equal to

$$(16) \quad I = \frac{V_Z}{R_p + \frac{1}{j\omega C_p}}.$$

Determining the voltage modules in the second balancing step is as difficult as in the first, and here the analysis is problematic, too.

The measured dielectric loss factor after the second balancing step can be determined from the relationship.

$$(17) \quad \tan \delta_X = \frac{R_{CC'}}{\sqrt{R^2 - (R_{CC'})^2}},$$

For low-loss capacitors, equation (17) can be simplified to an approximate form

$$(18) \quad \tan \delta_X \approx \frac{R_{CC'}}{R}.$$

### Simulation studies

As can be seen from the previous point, the analytical calculation of modules and analysis of the measurement process is complicated; therefore, the best way to assess the operation of the system and its properties is a simulation study. The LTspice tool was used for simulation studies [3].

The conclusion from previous work was the possibility of using the discussed system to measure the dielectric loss coefficient of insulation of power cables. Therefore, it was decided to adopt the parameters of the tested object typical for such applications. The following assumptions were made:

- serial model of the tested object,

- bridge supply voltage:  $V_Z = 10 \text{ V}$ ,
- measuring frequency of bridge supply voltage: 50 Hz,
- capacity of the tested object:  $10 \text{ nF} \dots 1 \mu\text{F}$ ,
- loss coefficient  $\tan \delta_X$  of the object under test:  $10^{-2} \dots 10^{-4}$ .

For such an object, the resistance of  $R_X$  ranges from approx.  $0.32 \Omega$  to approx.  $3.2 \text{ k}\Omega$  and the reactance of the imaginary part from approx.  $3.2 \text{ k}\Omega$  to approx.  $320 \text{ k}\Omega$ . It was assumed that the capacitance of the tested object would be equal to  $100 \text{ nF}$ , and the dielectric loss factor  $\tan \delta_X$  was assumed to be at the level of  $10^{-3}$ , which means the series resistance of the  $R_X$  series model of  $20 \Omega$ . For the purpose of simulation, the assumed resistance value  $R_2$  was  $40 \text{ k}\Omega$ .

Fig. 3 shows the layout diagram in the first balancing step in LTspice. The two halves of resistor  $R_2$  are designated  $R_{21}$  and  $R_{22}$  (as  $R/21$  and  $R/22$  in Fig. 4), which result from the properties of the LTspice schematic editor. The other markings correspond to the markings in Fig. 2.

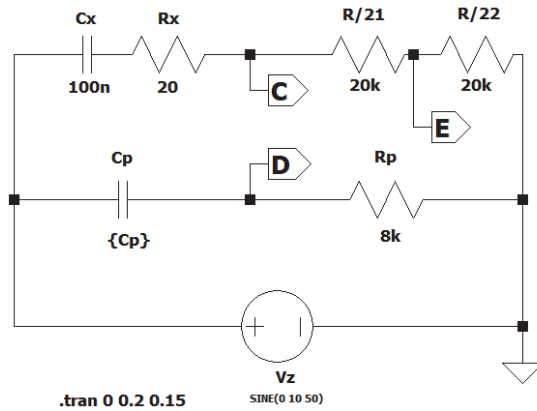


Fig. 4. Diagram of the circuit in the second balancing step

Fig. 5 shows an example of the dependence of the  $V_{DE}$  voltage module (amplitude) on the  $R_p$  resistor settings. It can be seen that around the first equilibrium (8) this relationship is approximately linear. It can also be seen that it is possible to achieve an undesirable false equilibrium. However, this possibility can be easily detected by observing the system's response to changes in adjustable resistance. As long as the  $V_{DE}$  voltage increases as the resistance decreases, it will mean that it is approaching a false equilibrium. The equilibrium state in the first step is achieved for the resistor setting  $R_p$  equal to  $8 \text{ k}\Omega$ .

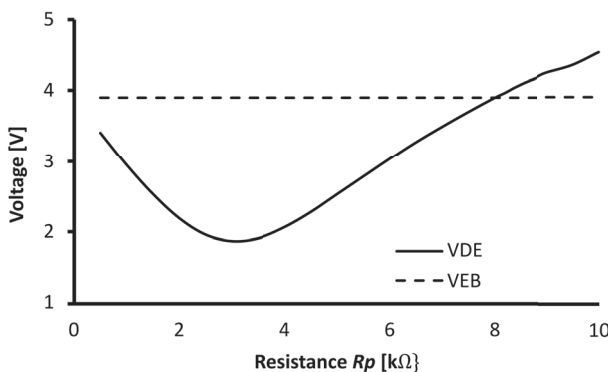


Fig. 5. Dependence of the  $V_{DE}$  voltage on resistor settings  $R_p$

Fig. 6 shows the layout diagram in the second balancing step. In the figure, point C' is marked as C1. As in the diagram in Fig. 4, this is due to the properties of the LTspice

schematic editor.

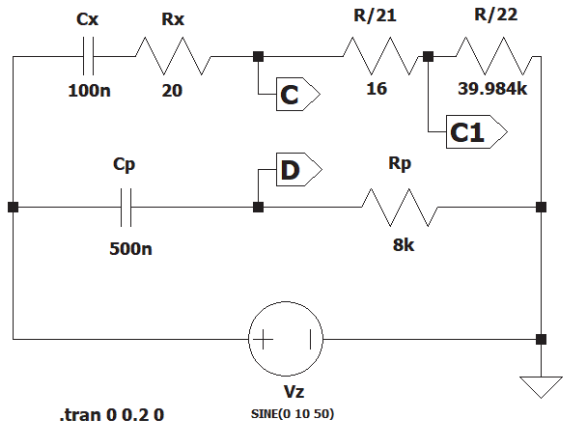


Fig. 6. Diagram of the circuit in the second balancing step

Fig. 7 shows the dependence of the  $R_{CC1}$   $V_{CD}$  voltage on the resistor settings. It can be seen that near the second equilibrium state, the voltage modulus  $V_{CC}$  depends approximately linearly on the settings of the resistor  $R_{CC1}$ . The equilibrium state in the second balancing step is achieved for a  $R_{CC1}$  resistor setting of  $15.8 \Omega$ .

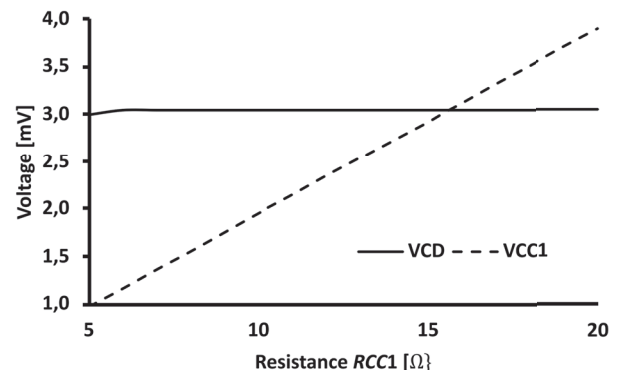


Fig. 7. Dependence of  $V_{CC'}$  voltage on resistor  $R_{CC1}$  settings

The values of the detectable system voltages are at the level of a few volts in the first balancing step and a few millivolts in the second step. This is due to the adopted value of the supply voltage. It can be seen that the result of measuring the dielectric loss factor requires knowledge of the resistance  $R$  and the resistance of the  $R_{CC'}$ . However, because the same current flows through both resistances, the measured  $\tan \delta$  determined as the voltage ratio of the corresponding resistances. The value of the dielectric loss factor calculated from Equation (18) is equal to the value assumed for the object under test. Among the elements that make up the bridge, the  $C_p$  capacitor plays an important role. The capacitor used as a capacitance standard may actually have a capacitance different from the assumed one and may show loss. Using the simulation model presented above, the influence of the non-ideality of the capacitor  $C_p$  on the value of the  $V_{DE}$  output voltage module was checked. Fig. 8 shows the dependence of the relative change in the  $V_{DE}$  voltage on the relative change in capacitance  $C_p$ . Changes in this capacity were assumed to be in the range of  $\pm 1\%$ .

These studies show that the influence of the capacitance value of the capacitor  $C_p$  on the measurement error may be negligible if a thermally stable capacitor is used as a standard and the value of the capacitance  $C_p$  is measured with appropriate accuracy.

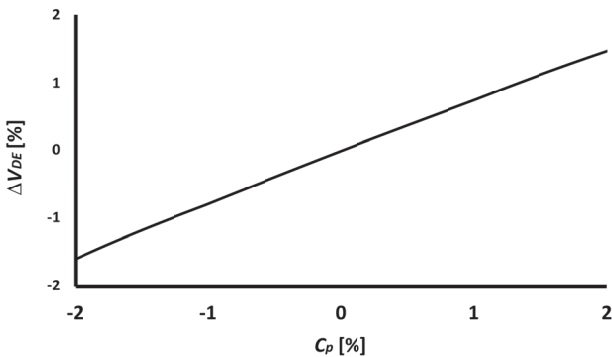


Fig. 8. Dependence of the change  $\Delta V_{DE}$  of the  $V_{DE}$  voltage module on changes  $\Delta C_p$  of capacitance values of capacitor  $C_p$  in the first measurement step

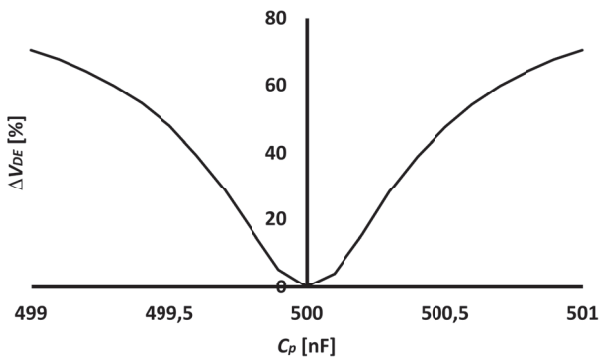


Fig. 9. Dependence of relative voltage changes  $\Delta V_{DC}$  on capacitance  $C_p$  in the second measurement step

In the next stage, the influence of the dielectric loss factor  $\tan \delta$  of the  $C_p$  capacitor was checked. In the first step of the measurement procedure, the non-zero  $\tan \delta$  can be neglected, the loss of standard has virtually no effect on the operation of the system, but in the second step its effect on the output voltage  $V_{CD}$  is visible. The characteristic of this voltage for different values of  $\tan \delta$  values ( $10^{-5}$ ,  $10^{-4}$ , and  $10^{-3}$ ) are shown in Fig. 9. The voltage amplitudes of  $V_{CD}$  have a value of 3.04 mV, 2.62 mV, 1.54 mV, respectively. For a  $C_p$  lossless capacitor, the  $V_{CD}$  amplitude is 3.08 mV. The

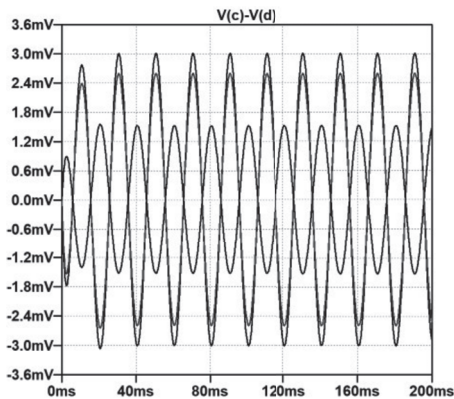


Fig. 10.  $V_{CD}$  voltage waveforms for different values of the dielectric loss coefficient  $\tan \delta$  in the second measurement step

effect of  $\tan \delta$  on the measurement result is significant. Analyzing the voltage dependence according to Fig. 7, it can be seen that for  $\tan \delta$  of the order of  $10^{-3}$ , to achieve the second equilibrium state, the output voltage should be changed from 2.64 mV to 3.08 mV by increasing the adjustable resistance of  $R_p$  by approximately 14%. Due to the linear dependence

of the measurement result on the value of the adjustable resistance  $R_p$ , this will also be the relative error in measuring the dielectric loss factor  $\tan \delta$ . Therefore, a capacitor with a  $\tan \delta$  factor less than  $10^{-4}$  should be used.

### Summary

This paper presents the results of research on a certain bridge system designed to measure the dielectric loss coefficient. This bridge is characterized by two consecutive balancing steps, with the modules of selected system voltages being detected. This type of circuits is quite rare [5].

Particular attention was paid to the system balance process. An attempt was made to derive equations describing the output voltages of the system, but due to the complex description, it was decided to simulate the operation of the system. The LTspice program was used a simulation, allowing for simple construction of the scheme and easy setting of system parameters. A serial model of the tested low-loss capacitor was assumed.

This paper presents the dependencies of the output voltages in both balancing steps. In a fairly wide range of settings of adjustable elements, the output voltages are proportional to the settings, which means a constant sensitivity of the system. In addition, these voltages are compared with constant reference values. Detection of both equilibrium states is easy, it is enough to measure the voltage modules, which in the case of sinusoidal voltages of the system can be achieved by measuring the RMS value of the voltages.

The influence of the capacitance standard present in the measurement process was also investigated. This standard should be chosen particularly carefully, because the impact of its nonideality, especially the loss factor  $\tan \delta$  on the measurement result can be significant.

Compared to typical balanced bridge systems, the presented solution is characterized by consistent maximum convergence. On the other hand, compared to quasi-balanced systems, they are characterized by ease of detecting highlighted states. These bridges do not require phase-sensitive detection, which can be difficult. The tested system allows us to measure the relation of impedance components, in this case the dielectric loss coefficient. The possibility of using a system to measure the quality factor of the coils should be considered.

**Authors:** Adam Cichy, PhD, DSc EE, Silesian University of Technology, Department of Measurement Science, Electronics and Control, ul. Akademicka 10, 44-100 Gliwice, e-mail: adam.cichy@polsl.pl; Adam Pilśniak PhD, Silesian University of Technology, Department of Measurement Science, Electronics and Control, ul. Akademicka 10, 44-100 Gliwice, e-mail: adam.pilsniak@polsl.pl.

### REFERENCES

- [1] Toroński Z.: Pomiar kąta stratności izolacji metodą woltomierzową, Zeszyty Naukowe Politechniki Śląskiej, Elektryka. Z. 3, nr 8, (1956). Wydawnictwo Politechniki Śląskiej, Gliwice, s. 101-102.
- [2] Cichy A.: Pomiar współczynnika strat dielektrycznych metodą dwóch woltomierzy, Przegląd Elektrotechniczny, 2022, vol. 98, nr 11, s.205-208. DOI:10.15199/48.2022.11.
- [3] [web page] <https://www.analog.com/en/design-center/design-tools-and-calculators/ltpspice-simulator.html>.
- [4] Karandeev K. B.: Bridge and potentiometer methods of electrical measurements. Peee Publishers, 1966.
- [5] Raouf M.H.A., Kim K-T., Kim D. B., Kim M-S.: A Simple Double-Balance Impedance Bridge for Routine Calibrations, IEEE. DOI:10.1109/CPEM.2012.6251130, (2012). Conference on Precision Electromagnetic Measurements, Washington, DC, USA, s.716-717.